Available online at www.sciencedirect.com
ScienceDirect
International Journal of Thermal Sciences 47 (2008) 1658–1664
International Journal of Thermal Sciences
www.elsevier.com/locate/ijts

Influence of surfactant on friction pressure drop in a manifold microchannel ☆

Guodong Xia [a,*], Qiming Liu [a], Jingzhi Qi [a], Jinliang Xu [b]

[a] *Key Laboratory of Enhanced Heat Transfer and Energy Conservation, Ministry of Education, College of Environmental and Energy Engineering, Beijing University of Technology, Beijing 100022, PR China*
[b] *Micro Energy System Laboratory, Guangzhou Institute of Energy Conversion, Chinese Academy of Science, Nengyuan Road, Guangzhou 510640, PR China*

Received 8 January 2007; received in revised form 24 January 2008; accepted 25 January 2008

Available online 14 March 2008

Abstract

Manifold microchannel (MMC) heat sinks have many advantages on low thermal resistance, compact structure, small amount of coolant, low flow rate, uniform temperature distribution along the flow direction, etc. However, a high pressure drop is needed due to the small channel size used thus the pumping power is increased. Here we study the effect of surfactant on friction pressure drop in a specifically designed manifold microchannel heat sink. The microchannel has a cross section of 100 microns by 300 microns with a length of 10.0 mm. An anionic surfactant of 100 ppm Sodium Dodecyl Sulphate (SDS with 95% purity grade) aqueous solution and a new type of 300 ppm green non-ionic surfactant of Alkyl Polyglycoside (APG1214 with 98% purity grade) aqueous solution are used as the working fluids. It is found that the drag reductions are dependent on the flow velocities and the fluid temperatures. The drag reduction is not significant for laminar flow, but it is increased in the transition flow regime. The temperature rise can promote the drag reductions in the presence of SDS and APG. It is shown that the APG is better than the SDS regarding the drag reductions at high temperatures.

Keywords: Drag reduction; Surfactant; Manifold microchannel

1. Introduction

The Drag Reduction (DR) is a possible measure to reduce the friction pressure drop in pipelines. The addition of a Drag Reducing Agent (DRA) to a fluid in pipes results in a decrease of the pressure drop for a fixed flow rate, or an increase of the flow rate for a fixed pressure drop. The effect of such additives has been widely studied in macroscale in the past years. Several mechanisms have been proposed trying to explain the observed phenomena [1]. The review papers can be found in Virk [2], Hoyt [3], Lumley [4], Berman [5] and Gyr and Bewersdorff [6].

Li et al. [7] found that there are an upper critical temperature and a Reynolds number beyond which the DR surfactant has no effect on the flow and the heat transfer is deteriorated. Usui et al. [8] developed a scale law by introducing the turbulence model for the Drag Reduction flow, which could estimate the pipe diameter effect with the diameter ranging from 11 to 150 mm. Suksamranchit et al. [9] studied the turbulent DR flow by shearing the two opposite plates. The wall shear stress can be decreased for three kinds of additives and mixtures. Their studies identified the effects of molecular weight and concentrations on the drag reductions. The experimental study on the surfactant DR flow can also be found in Zakin et al. [10].

Several researchers explain the drag reduction mechanism using the theory of the DRA macromolecule elasticity. The DRA molecules become lengthened in the high elongational strain turbulent flow. This theory gives a good explanation that the drag reduction does not exist for laminar flow [11]. It is proposed that the DRA molecules are more active in the buffer

☆ Research is supported by the National Natural Science Foundation of China (50476035), the Beijing Natural Science Foundation (3052004) and the Science & Technology Development Project of Beijing Education Committee (KZ200710005001).
* Corresponding author.
E-mail address: xgd@bjut.edu.cn (G. Xia).

1290-0729/$ – see front matter © 2008 Published by Elsevier Masson SAS.
doi:10.1016/j.ijthermalsci.2008.01.014

Nomenclature

C_{fl}	laminar coefficient for channel flow
C_{ft}	turbulent coefficient for channel flow
D_h	hydraulic diameter ..... m
DR	drag reduction ..... %
f	friction factor
f_{with}, $f_{without}$	friction factors with and without drag reducing agent, respectively
H_c	depth of microchannel ..... μm
L_c	length of microchannel ..... m
Δp	pressure drop ..... Pa
Δp_{with}, $\Delta p_{without}$	pressure drop with and without drag reducing agent, respectively ..... Pa
q_V	volumetric flow rate ..... $m^3\,s^{-1}$
Re	Reynolds number
Re_c	critical Reynolds number at which the flow switches to the transition regime
u	average velocity of coolant ..... $m\,s^{-1}$
W_c	microchannel width ..... μm
α	aspect ratio of microchannel
γ	kinematic viscosity ..... $m^2\,s^{-1}$
ρ	density of coolant ..... $kg\,m^{-3}$

zone located between the viscous sub-layer adjacent to the wall surface and the turbulent core of the flow [12].

Wilson [13] proposed that the drag reduction is related to the thickening of the near-wall sub-layer for the laminar flow. Even though he agreed that this mechanism can not explain the polymeric DRA flow in pipelines, he stated that DRA molecules can increase the elongational viscosity of the fluid, reducing the transport of both vorticity and momentum into the turbulent core, finally leading to the modification of the logarithmic velocity profile, which was first found by Virk et al. [14].

Li et al. [15] studied the turbulence structures for the Reynolds number dependent flow and demonstrated the dynamic processes of the shear induced flow structure across the flow passage. Based on the relationship between the Reynolds number and the drag reduction levels, the Cetyltrimethyl Ammonium Chloride (CTAC) solution flow is divided into four regimes. In their experiment, Sodium Salicylate (NaSal) was used to provide the counterions, and was added to the solution with the same weight concentration as that of CTAC.

Yu et al. [16] numerically studied the drag reduction turbulent flows using the surfactant additives. They found that the drag reduction is not only related to the reduction of the Reynolds shear stress but also related to the induced viscoelastic shear stress.

Many studies deal with the practical applications of DRAs. Wei et al. [17] studied the Ethoquad O12/NaSal surfactant Drag Reduction flow in a two-dimensional channel below freezing temperature to design an efficient cooling system. They found a complicated relationship between the mass fraction and temperature. A comprehensive review can be found in Sellin et al. [18], covering a wide range of technical fields.

Even though many studies have been performed at macroscale, little attention has been received at microscale. It is well known that microchannels can enhance heat transfer. But an important issue is the increased pressure drop when the channel size is significant decreased.

The present work is an attempt to identify the effect of the surfactant on the friction pressure drop in a microchannel heat sink. The DRAs used are the anionic surfactant of Sodium Dodecyl Sulphate (with 95% purity grade) aqueous solution and the green non-ionic surfactant of Alkyl Polyglycoside (APG1214 with 98% purity grade) aqueous solution. The temperature effect on the drag reduction of the SDS and the APG is also taken into consideration.

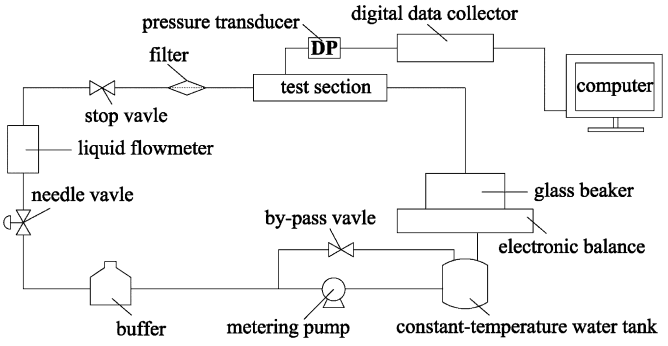

Fig. 1. Experimental setup.

2. Experimental setup and procedures

2.1. The experimental setup

The experimental setup consists of three major subsystems: (a) the test section, (b) the flow subsystem, and (c) the instrumentation and data acquisition subsystem. Fig. 1 shows the experimental setup. The working fluid was stored in a well temperature controlled tank. It was pumped by a metering pump and flowed successively through a buffer, a liquid valve, a calibrated liquid flow meter, a 10 μm filter and the test section, and was finally collected by a glass beaker. The pressure drop across the test section was measured. The mass flow rate was determined by weighing the mass increment over a given period of time with a precision electronic balance.

As shown in Fig. 2, the test section consists of a microchannel heat sink and two opposite plates, allowing the fluid transport through the microchannel heat sink and the pressure drop measurement. The microchannel heat sink was bonded by the top and bottom non-oxygen copper plates.

The top plate was made of a transparent Plexiglass so that the flow visualization can be performed. The bottom plate was also made of a transparent Plexiglass and three circular manifold channels with a depth of 8.0 mm and a diameter of 1.0 mm

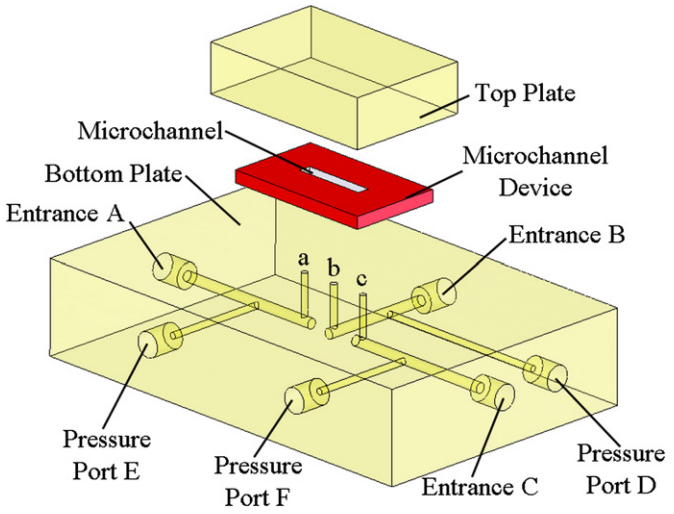

Fig. 2. Test section.

are drilled on it. As shown in Fig. 2, they are vertical to the microchannel and connect to the middle point (b) and two ends (a) and (c) of the microchannel, respectively. In order to connect the manifold channels to three entrances (the entrances A, B and C in Fig. 2), three 20.0 mm long circular channels with a diameter of 2.0 mm were processed horizontally. Finally, three pressure ports (D, E, and F in Fig. 2) were made on the bottom plate for the Rosemount3051C pressure transducer.

Two pieces of Plexiglass plates housed a number of bolts for fluidic sealing and the easy positioning of microchannel. The microchannel device was compressed against the bolts by the top and the bottom plates to forge the fluidic seals. This setup ensured hermetic sealing and offered access to the fluidic connections (inlet, outlet, and pressure ports) of the micro device through the bottom plate.

2.2. Experimental procedure

The microchannel has a cross section of 100 microns width and 300 microns depth with the length of 10.0 mm. Before the experiments, the pressurized nitrogen gas was introduced for half hour to ensure that there was no leakage of the test section. The deionized water, SDS aqueous solution and APG aqueous solution were used as the working fluids, respectively. The temperature of the working fluid was controlled by the constant temperature tank. The inlet and outlet fluid temperatures were measured by the precision thermocouples with the diameters of 0.3 mm and the uncertainty of 0.2 °C.

The pressure drop of the deionized water flowing from the port B to the ports A and C, and from the ports A and C to the port B, was tested (see Fig. 2), to identify the flow direction effect on the pressure drop in the manifold microchannel.

The next step was to study the pressure drop in the microchannel. The total pressure drop consists of three components: (1) pressure drop in the microchannel, (2) pressure drop in the manifolds, and (3) pressure drop due to the abrupt change of the channel cross section area and the sharp change of the flow directions. It is noted that only the first part can be used to compute the friction factor in the microchannel. In the test section, the majority of total pressure drop is in the microchannel. So the following experimental procedure was taken:

The deionized water was flowing through the test section from the entrance A to C by closing the entrance B. Thus the pressure drop between the port E and the port F (Δp_{EF}) can be obtained, which consists of three parts: the pressure difference Δp_{Ea} between the port E and the spot a, the pressure difference Δp_{ac} between the spots a and c, and the pressure difference Δp_{cF} between the spot c and the port F. The following expression exists

$$\Delta p_{EF} = \Delta p_{Ea} + \Delta p_{ac} + \Delta p_{cF} \tag{1}$$

After the above procedure, the deionized water was flowing through the test section from the entrance A to B by closing the entrance C. Similarly, the pressure drop between the port E and the port D (Δp_{ED}) can be obtained, consisting of three parts: the pressure difference Δp_{Ea} between the port E and the spot a, the pressure difference Δp_{ab} between the spots a and b, and the pressure difference Δp_{bD} between the spot b and the port D.

$$\Delta p_{ED} = \Delta p_{Ea} + \Delta p_{ab} + \Delta p_{bD} \tag{2}$$

where

$$\Delta p_{ac} = \Delta p_{ab} + \Delta p_{bc} \tag{3}$$

It is noted that the local pressure drops in the bends are contained in Δp_{Ea}, Δp_{cF}, and Δp_{bD}. In the present experimental condition, more than 50% of the pressure drop is in the test section of the microchannel. As noted previously, the structure between the spot c to the port F is same as that between the spot b to the port D. Thus it can be concluded that Δp_{cF} in Eq. (1) and Δp_{bD} in Eq. (2) are equal at the same flow rate. The pressure drop between the spots b and c can be obtained as follows

$$\Delta p_{bc} = \Delta p_{EF} - \Delta p_{ED} \tag{4}$$

The final step was to study the influence of the surfactant on the friction pressure drop in the microchannel. The similar procedure was applied as above.

Since the aqueous surfactant solution can cause a lot of foam during the flowing, the concentration of surfactant solution will be decreased gradually, affecting the experimental accuracies if the surfactant solution was recycled in the loop system. Thus the surfactant solution was discarded after it flows out of the test section, avoiding the complicated evaluating the concentration changes of solutions affected by some uncontrolled factors such as forming.

In the present work, the flow rate for each working fluid is in the range from 1.67×10^{-9} to 1.33×10^{-6} m^3 s^{-1}. Correspondingly the flow velocities are varied from 0.28 to 22.22 m s^{-1} and the Reynolds numbers from 50 to 3500.

The inlet fluid pressure was measured by a Rosemount3051C pressure transducer and the outlet fluid pressure was kept at the atmospheric pressure in the experiments. All the pressure and temperature signals were collected by a HP34970A data acquisition system. The flow rate and the pressure drop have the uncertainties of 0.5 and 1.5%, respectively. The fluctuation of pressure drop is very small within the range less than 2%.

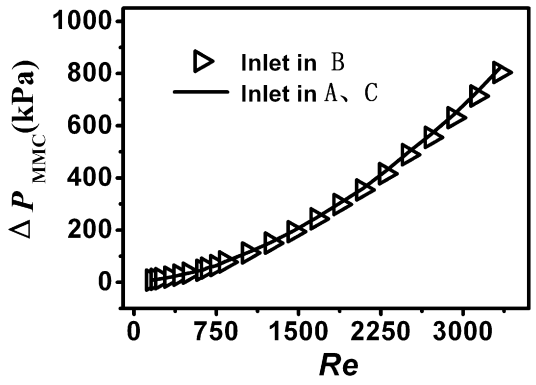

Fig. 3. Relationship between experimental Δp_{MMC} and Re at two kinds of flow directions.

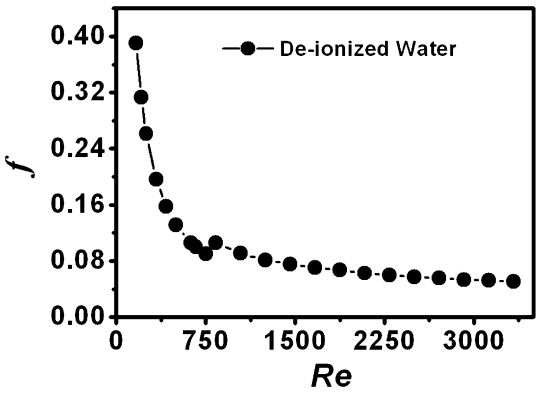

Fig. 4. Relationship between experimental friction factor f and Reynolds number Re.

3. Results and discussion

3.1. Influence of flow direction on pressure drop in the manifold microchannel

As noted previously, the effect of flow direction on pressure drop is studied in the present work. Fig. 3 shows the measured pressure drops versus the Reynolds number for two flow directions. The hydraulic diameter of the microchannel is used to characterize the flow. It is seen that the measured results are almost the same for the two flow directions with the difference less than 3%, indicating little effect of flow direction on the pressure drops.

3.2. Pressure drop in the microchannel

The pressure drop across the whole manifold microchannel consists of three components, which are that consumed in the microchannel, in the manifolds, and produced due to the abrupt change of the cross section areas and the hard edge. The pressure drop in the microchannel can be obtained by removing the last two terms of pressure drops.

The mean flow velocity, hydraulic diameter, and the Reynolds number are computed as

$$u = q_V/(W_c \cdot H_c) \tag{5}$$

$$D_h = 2W_c H_c/(W_c + H_c) \tag{6}$$

$$Re = u D_h/\gamma \tag{7}$$

where γ is the kinematic viscosity of the solvent. It is convenient to use the solvent viscosity instead of the solution viscosity for the drag reduction flow. As indicated by Virk [2], the shear-thinning behavior of dilute polymeric and surfactant solutions have little effects on the gross flows.

$$f = 2D_h \Delta p/\left(\rho L_c u^2\right) \tag{8}$$

Eq. (8) is used to obtain the experimental decided friction factor.

The friction factor f can be calculated using the available correlations. For laminar flow in rectangular channels, the laminar coefficient was proposed by Cornish [19]

$$C_{\mathrm{fl}} = \frac{96}{(\alpha+1)^2}\left(1 - \frac{192\alpha}{\pi^5}\sum_{n=1}^{\infty}\frac{\tanh((2n-1)\pi/2\alpha)}{(2n-1)^5}\right)^{-1} \tag{9}$$

where α is the aspect ratio of the rectangular channel. $C_{\mathrm{fl}} = f \cdot Re$ is the laminar coefficient for rectangular channel flow.

For the turbulent friction factor in a non-circular channel, Sadatomi et al. [20] took account of channel geometry and proposed the following empirical relationship between the laminar coefficient C_{fl}, which is given by Eq. (9), and the turbulent coefficient C_{ft}:

$$\frac{C_{\mathrm{ft}}}{C_{\mathrm{ft,pipe}}} = \left(0.0154\frac{C_{\mathrm{fl}}}{C_{\mathrm{fl,pipe}}} - 0.012\right)^{1/3} + 0.85 \tag{10}$$

where $C_{\mathrm{ft}} = f \cdot Re^{0.25}$ is the turbulent coefficient for rectangular channel flow. $C_{\mathrm{ft,pipe}} = 0.3164$ is the turbulent coefficient in circular pipes. C_{fl} is given by Eq. (9) for rectangular channel flow. $C_{\mathrm{fl,pipe}} = 64$ is the laminar coefficient in circular pipes.

Fig. 4 shows the experimental friction factor f versus the Reynolds number. It is seen that the laminar flow is ensured when Reynolds number is smaller than 800. Beyond the Reynolds number of 800, the flow is in the transition regime. In macroscale rectangular channels, Cornish [19] provided the first indication that the critical Reynolds number (Re_c) for transition increases with increasing aspect ratio. He reported that $Re_c = 2225$ in a macroscale rectangular channel with aspect ratio of 2.92. It seems that the critical Reynolds number at which the flow switches to the transition regime in microchannels is smaller than that in macroscale rectangular channels. Fig. 5 shows the comparison between the computed friction factor and the experimental data. The measured friction factors match the computed values using Eq. (9) in the laminar flow regime. Their differences are less than 5%. When the Reynolds numbers are larger than 800, the measured friction factors are larger than those computed using Eq. (10) for the fully developed turbulent flow. And the experimental data approaches Eq. (10) as Re increases supporting the transition regime hypothesis. It indicates that the flow of $Re = 800$–3500 is in the transition regime.

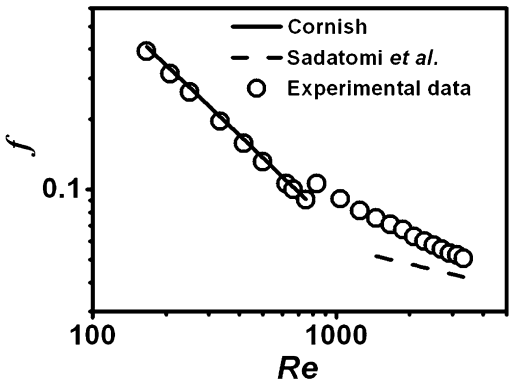

Fig. 5. Comparison between calculated friction factor and the experimental data.

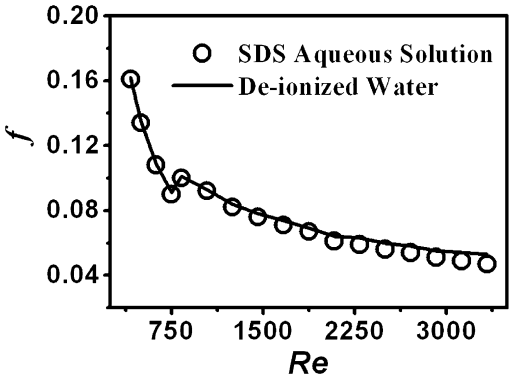

Fig. 6. Influence of the SDS on friction factor (20 °C).

3.3. Influence of SDS surfactant on drag reductions at different temperatures

Fig. 6 shows the comparison of the friction factors with and without the SDS surfactant at the room temperature. It is seen that the SDS has little effect on the flow switch from the laminar flow to the transition flow, which occurs at the Reynolds number of 800. In the laminar flow regime, the friction factor f with the SDS surfactant is close to that without the SDS. In the transition flow regime, however, the friction factor f with the SDS begins to be smaller than that without the SDS. Their difference is increased with increasing the Reynolds number.

Fig. 7 shows the influence of temperature on the DR effect of the SDS surfactant. The friction factor f decreases with increasing the temperature at any prescribed *Re* in the transition flow regime, indicating that the rise of temperature can increase the DR effect of the SDS. The higher the Reynolds number is, the greater the DR effect of the SDS surfactant is. It is noted that the effect of surfactant solution and the pure water data are compared with each other based on the same temperature. This is true for the following figures and elsewhere.

3.4. Influence of APG surfactant on drag characteristics at different temperatures

The 300 ppm APG1214 aqueous solution is used to study the influence of the APG surfactant on pressure drop at different

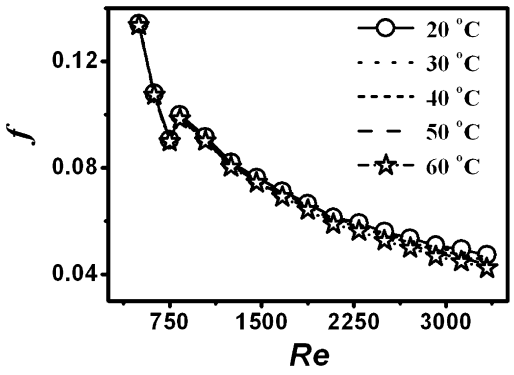

Fig. 7. Influence of temperature on DR effect of the SDS surfactant.

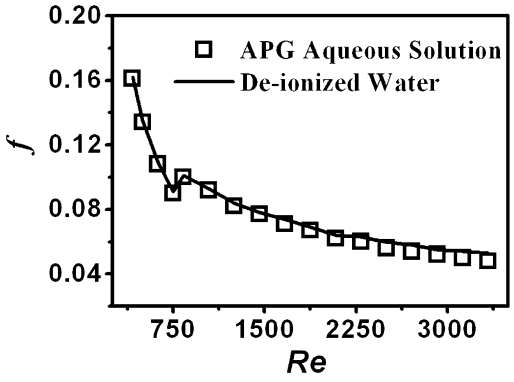

Fig. 8. Influence of the APG surfactant on friction factor (20 °C).

temperatures. The general formula of APG is $(G)nOR$, where G is carbohydrate unit containing 5–6 carbon atoms, and n is the number of carbohydrate units, and R is Alkyl. In APG1214, the Alkyls contain 12–14 carbon atoms.

Fig. 8 shows the comparison between the experimental friction factor f with and without the APG surfactant at the room temperature. Similar to the SDS surfactant, the addition of the APG has little effect on the flow switch from the laminar flow to the transition flow. In the laminar flow regime, the friction factor f with the APG is close to that of pure water. When the flow is in the transition flow regime, the drag reduction effect of the APG surfactant can be observed, especially for the higher Reynolds numbers.

Fig. 9 shows the influence of the temperature on the drag reduction of the APG aqueous solution in the microchannel. In the transition flow regime, the friction factor is decreased with increasing the temperature at the given *Re*, indicating that the rise of temperature can increase the DR effect of the APG. The higher the Reynolds number is, the greater the DR effect of the APG surfactant is.

3.5. Drag Reduction (DR)

It is common to compare the pressure gradients of a system with and without drag reduction agent (DRA). Savins [21] is the first to use the term "Drag Reduction" with the definition as

$$\mathrm{DR}\% = \left[1 - \frac{\Delta p_{\mathrm{with}}}{\Delta p_{\mathrm{without}}}\right] \times 100\% \tag{11}$$

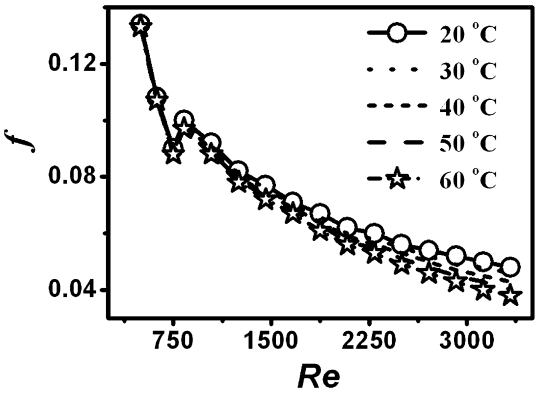

Fig. 9. Influence of temperature on DR effect of the APG surfactant.

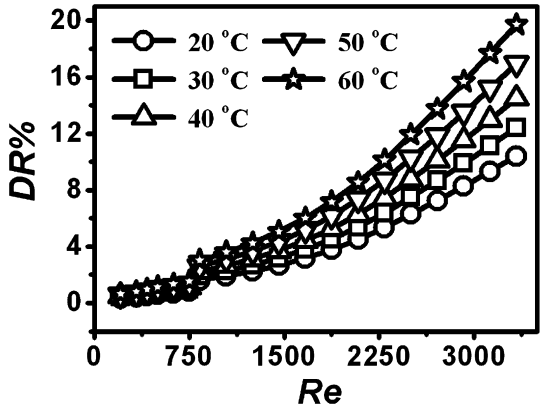

Fig. 10. Influence of the SDS surfactant on drag reduction at different temperatures.

where Δp_{with} and $\Delta p_{\text{without}}$ are the friction pressure drops for the internal flow at a given flow rate, with and without drag reducing agent, respectively.

This can also be written in terms of friction factors:

$$\text{DR}\% = \left[1 - \frac{f_{\text{with}}}{f_{\text{without}}}\right] \times 100\% \tag{12}$$

where f_{with} and f_{without} are the friction factors for the internal flow at a given flow rate, with and without drag reduction agent, respectively.

The DR% with the SDS or the APG can be calculated based on the experimental results. Figs. 10 and 11 show the influence of the SDS and the APG on the drag reduction at different temperatures, respectively. Seeing from Figs. 10 and 11 is that the drag reductions are very small in the laminar flow regime for any kind of surfactant used. However, the drag reductions begin to increase beyond the Reynolds number of 1000 in the transition flow regime. This finding is in accordance with the results in the macroscale size channels [22]. It is also seen from Figs. 10 and 11 that the increase of temperatures can yield high drag reductions.

Figs. 12 and 13 are used to present the comparisons of the drag reduction effects of the SDS and APG. It is found that the SDS is better than the APG on the drag reduction effect at the room temperature of 20 °C. However, the APG is better than the SDS at the temperature of 60 °C, indicating the strong temperature effect.

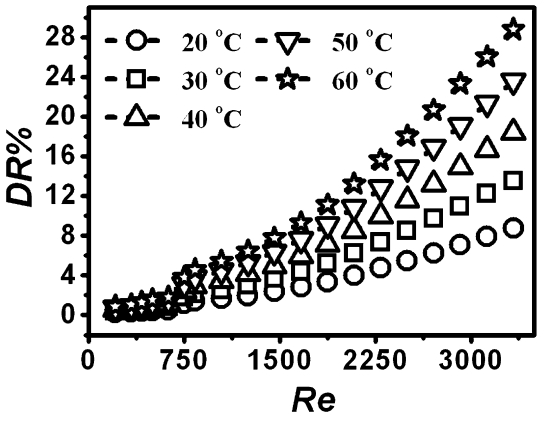

Fig. 11. Influence of the APG surfactant on drag reduction at different temperatures.

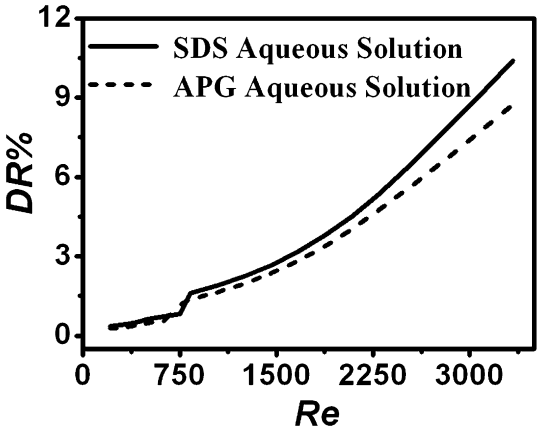

Fig. 12. Comparison between drag reductions of the SDS and the APG (20 °C).

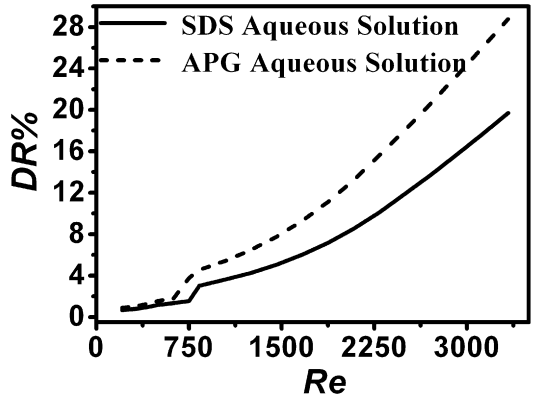

Fig. 13. Comparison between drag reductions of the SDS and the APG (60 °C).

We tested two kinds of surfactant solutions for the drag reductions in the present paper. There are much more effective surfactant agents in the literatures, which will be recommended for the future experiments.

4. Conclusions

We study the influence of the surfactant on the pressure drops experimentally in this paper. The deionized water, the 100 ppm Sodium Dodecyl Sulphate (SDS) aqueous solution

and the 300 ppm Alkyl Polyglycoside (APG) aqueous solution are used as the working fluids. The following conclusions can be drawn:

(1) The flow directions have little effect on the pressure drops in the manifold microchannel at any conditions.
(2) The critical Reynolds number (Re_c) at which the flow switch occurs from the laminar flow to the transition flow is identified to be about 800, which is smaller than that in macroscale rectangular channels.
(3) The influence of the surfactant on the pressure drops depends on the flow regime. In the laminar flow regime, the addition of the SDS or the APG has little effect on pressure drops. In the transition flow regime, the drag reduction effect is prominent.
(4) The influence of surfactant on pressure drops also depends on the temperature of the working fluids. The drag reductions of both surfactants are increased with increasing the temperatures at any Reynolds numbers in the transition flow regime or for the higher Reynolds numbers. The APG has better drag reduction effect than the SDS at higher temperatures.

References

[1] P.D. Manfield, C.J. Lawrence, G.F. Hewitt, Drag reduction with additives in multiphase flow: A literature survey, Multiphase Sci. Tech. 11 (3) (1999) 197–221.
[2] P.S. Virk, Drag reduction fundamentals, AIChE J. 21 (4) (1975) 625–656.
[3] J.W. Hoyt, The effect of additives on fluid friction, J. Basic Eng. Trans. ASME Ser. D 94 (2) (1972) 258–285.
[4] J.L. Lumley, Drag reduction by additives, Ann. Rev. Fluid Mech. 1 (1969) 367–384.
[5] N.S. Berman, Drag reduction by polymers, Ann. Rev. Fluid Mech. 10 (1978) 47–64.
[6] A. Gyr, H.W. Bewersdorff, Drag Reduction of Turbulent Flows by Additives, Kluwer Academic Publishers, Dordrecht, The Netherlands, 1995.
[7] F.C. Li, Y. Kawaguchi, K. Hishida, Investigation on the characteristics of turbulence transport for momentum and heat in a drag-reducing surfactant solution flow, Phys. Fluids 16 (9) (2004) 3281–3295.
[8] H. Usui, T. Itoh, T. Saeki, On pipe diameter effects in surfactant drag-reducing pipe flows, Pheologica Acta 37 (2) (1998) 122–128.
[9] S. Suksamranchit, A. Sirivat, A.M. Jamieson, Polymer-surfactant complex formation and its effect on turbulent wall shear stress, J. Colloid Interface Sci. 294 (1) (2006) 212–221.
[10] J.L. Zakin, Y.Y. Qi, Y. Zhang, Recent experimental results on surfactant drag reduction, in: Proceedings of the 4th ASME/JSME Joint Fluids Engineering Conference, vol. 2, Part A, 2003, pp. 729–734.
[11] R.H.J. Sellin, J.W. Hoyt, O. Scrivener, The effect of drag-reducing additives on fluid flows and their industrial applications. Part I: Basic aspects, J. Hydr. Res. A 20 (1) (1982) 29–68.
[12] R.C. Little, R.J. Hansen, D.L. Hunston, O.K. Kim, R.L. Patterson, R.Y. Ting, The drag reduction phenomenon, observed characteristics, improved agents and proposed mechanisms, Ind. Eng. Chem. Fundam. 14 (4) (1975) 283–296.
[13] C. Wilson, Two mechanisms for drag reduction, in: Proc. 4th Int. Conf. Drag Reduction, Davos, Switzerland, July 31–August 3; republished in: R.H.J. Sellin, R.T. Moses (Eds.), Drag Reduction in Fluid Flows, Techniques for Friction Control, Ellis Horwood Publishers, Chichester, UK, 1989, pp. 1–8.
[14] P.S. Virk, H.S. Mickley, K.A. Smith, The ultimate asymptote and mean flow structure in Toms' phenomenon, J. Appl. Mech. Trans. ASME 37 (2) (1970) 488–493.
[15] F.C. Li, Y. Kawaguchi, T. Segawa, K. Hishida, Reynolds-number dependence of turbulence structures in a drag-reducing surfactant solution channel flow investigated by particle image velocimetry, Phys. Fluids 17 (7) (2005) 1–13.
[16] Y. Yu, B. Kawaguchi, DNS of drag-reducing turbulent channel flow with coexisting Newtonian and non-Newtonian fluid, J. Fluids Eng. Trans. ASME 127 (5) (2005) 929–935.
[17] J.J. Wei, Y. Kawaguchi, Experimental study of surfactant drag-reducing flow in 2-D channel at subzero temperature, Hsi-An Chiao Tung Ta Hsueh (Journal of Xi'an Jiaotong University) 40 (1) (2006) 79–83.
[18] R.H.J. Sellin, J.W. Hoyt, O. Scrivener, The effect of drag-reducing additives on fluid flows and their industrial applications. Part II: Present applications and future proposals, J. Hydr. Res. B 20 (3) (1982) 235–292.
[19] R.J. Cornish, Flow in a pipe of rectangular cross-section, Proc. Royal Soc. London Ser. A 120 (1928) 691–700.
[20] Y. Sadatomi, Y. Sato, S. Saruwatari, Two-phase flow in vertical noncircular channels, Int. J. Multiphase Flow 8 (1982) 641–655.
[21] J.G. Savins, Drag reduction characteristics of solutions of macromolecules in turbulent pipe flow, Soc. Petrol. Eng. J. 4 (1964) 203.
[22] D.A. Storm, R.J. McKeon, H.L. McKinzie, C.L. Redus, Drag reduction in heavy oil, in: Energy Sources Tech. Conf. & Exhibition, ASME, Report 6672, 1999.